Pattern morphologies in thin liquid films

Voicu, Nicoleta Elena

CHAPTER

SEVEN

ALIGNMENT OF LAMELLAR BLOCK COPOLYMERS VIA ELECTROHYDRODYNAMIC–DRIVEN MICROPATTERNING

The combination of top–down approaches with block copolymer bottom–up self–assembly in a single processing step [102–104] has received increasing attention because of its potential use for sub–100 nm lithography. This so far unachieved principle employs block copolymer self–assembly for the controlled formation of 10–nm-sized patterns, which are interfaced by larger structures providing the addressability of self–assembled nano–devices. The successful implementation of such a device requires a simultaneous control over the self–assembly process and the large–scale structures. Both have been demonstrated individually in a number of ways, but their combination remains elusive.

7.1 Introduction

The alignment of microdomains perpendicular to the substrate is important because this is a typical requirement for nanotechnological applications [105] and can be achieved by the confinement of thin block copolymer films or the application of external fields, such as mechanical shear fields and electric fields. The resulting nanostructures which are accessible from the air surface can for example be partially degraded thereby serving as templates for metals [106] and semiconducting [107] nanowires.

The long–range lateral control over the orientation of block copolymer domains

in polymer melts and solutions has been demonstrated in a number of ways, such as the use of steady shear [108–110], capillary extrusion [111], and elongational flow [112,113]. The roll–casting of solutions [114–116] or shearing of block copolymer films with silicon rubber pads [117] also results in a long–range order of microphase separated block copolymer morphologies. The alignment of block copolymer morphologies using electric fields [118,119] is particularly interesting because of the level of control that can be achieved by this method. Since the domains follow the electric field lines [120–122] the local alignment of the microphase morphology both perpendicular [123, 124] and parallel [125–129] to the film–normal is possible. The long–ranged nature of electric field results in an equally long ranged alignment of the microphase morphology. Additionally, large–scale topographic structures can be generated in a controlled fashion by an electrohydrodynamic (EHD) film instability.

EHD pattern formation is a technique in which a liquid dielectric interface is destabilized by an electric field that is applied normal to this interface. In a homogeneous field, this gives rise to micrometer–sized columns with a well defined diameter and spacing [47, 49]. By using heterogeneous fields (generated e.g. by micro–patterned electrodes) nearly any pattern can be replicated into a homopolymer film [81]. Russell *et al.* used electrostatic forces to pattern block copolymer films with a cylindrical microphase morphology to create well–ordered patterns of columns, tens of micrometers in size [130].

7.2 Experimental

The relative PS–PMMA volume fraction of the used block copolymers was close to 50% leading to a lamellar microphase morphology in the bulk. Thin block copolymers films were spin–cast from toluene solutions with block copolymer concentrations of 2 to 3 wt %. Typical spinning speeds were 3000 to 8000 rpm resulting in film thicknesses between 100 and 200 nm. All silicon wafers were snow–jet cleaned prior to use. Top electrodes were planar silicon wafers or topographically structured surfaces. Silicon top electrodes were rendered hydrophobic by the deposition of a 1H,1H,2H,2H–perfluorodecyltrichlorosilane self–assembled monolayer to reduce the adhesion of block copolymer. To ensure a good electrical contact, the silicon substrates were coated on their backside with 2 nm Cr and 100 nm Au by thermal evaporation. ITO–coated glass slides were alternatively used as top electrodes. The block copolymer coated bottom electrode was loaded into the sample chamber, Fig. (7.1a), and the upper electrode was mounted on top of the polymer film with the polished side facing the film. The as–prepared samples were annealed at temperatures above the glass transition temperature of the two blocks ($T = 170\,^{\circ}\mathrm{C}$) or exposed to a well–controlled atmosphere of toluene vapor (a good solvent for both blocks) to induce mobility and facilitate equilibration. The solvent vapor pressure in the chamber was adjusted using a home–made apparatus [98, 99, 131]. Mass–flow controllers (MKS Instruments Model 1179A with a PR4000F readout) regulated the flux of the carrier gas N_2 through two lines. In one line, the N_2 was bubbled through a solvent–filled bot-

tle resulting in a solvent–saturated gas stream. Both streams were mixed and passed through the sample chamber. The flow rates were individually regulated to values between 1 and 20 $cm^3 min^{-1}$. The vapor pressure in the mixing chamber can be estimated by the ratio of the saturated (p_{sat}) to dry (p) gas flow rates as determined by the flow–meter readout. The films were allowed to swell in the controlled solvent atmosphere until an equilibrium film thickness was reached. The polymer concentration in the equilibrated film at a set vapor pressure is given by $\phi = d_0/d$, with d_0 and d the dry and swollen film thicknesses, respectively (assuming additivity of the partial volumes of polymer and solvent). At a vapor pressure of $p_{tol} = 0.85 p_{sat}$ the films swell to 1.7 times their dry thickness resulting in polymer concentrations of $w_p = 0.58$. This concentration is well above the order–disorder transition for the diblock copolymers.

Instead of using spacers to control the air gap [100], the two surfaces were brought directly into contact with each other. A finite air gap arises from deviations in the planarity of the two surfaces and from a low concentration of defects (dust particles) that are trapped between the two plates. In the case of temperature annealing a voltage of 40–80 V was applied between the two plates and the temperature of the device was raised to 170 °C for periods of time ranging from several minutes to several hours. Cooling the sample down to room temperature and removing the electric field terminated the experiment. For the solvent–vapor experiments the block copolymers were allowed to swell to their equilibrium thickness – typically ≈ 20 minutes [76] and voltages of 40–80 V were applied across the sandwich for several periods of time. The removal of the solvent was performed by passing dry N_2 through the sample chamber. After this quenching process the electric field and the top wafer were removed. The topography of the micro–patterned diblock copolymer films was analyzed by optical microscopy and Tapping Mode Atomic Force Microscopy (AFM, Digital Instruments D3100). AFM was also used to determine film thicknesses, which allows the calculation of the plate spacing h and the air gap h–d. To elucidate the lamellar microdomain structures within the columnar structures field emission scanning electron microscopy (FESEM, LEO 1530) was performed. The typical preparation of the samples for SEM was as follows: UV radiation under vacuum for 10 minutes, rinsing in acetic acid for 5 minutes and washing with Millipore water to selectively remove the PMMA block within the block copolymer structures. Prior to SEM imaging, a thin layer of gold, ≈ 5 nm, was evaporated onto the block copolymer surface to prevent charging of the polymer during imaging. The simulations were done in Comsol Multiphysics using the finite element method to solve for the electric field.

7.3 Results and discussion

7.3.1 Lamellar block copolymers alignment via EHD driven micropatterning

Here we discuss the interplay of EHD structure formation with the structural control over block copolymer microphase morphology. Upon temperature or solvent va-

por annealing, initially flat block copolymer films are destabilized by electric fields leading to the formation of micrometer sized pillars perpendicular to the substrate. This coarse pattern has a further substructure which arises from the alignment of the microphase–separated lamellar block copolymer morphology parallel to the electric field lines, i.e. parallel to the axis of the columns, Fig. (7.1b).

The experimental setup is summarized in Fig. (7.1a). Films consisting of polystyrene (PS)-*b*- poly(methyl methacrylate) (PMMA) block copolymers (Table 3.2) were confined between two electrodes, leaving an air gap. The samples were annealed either by raising the temperature above the glass transition temperature of the two constituent components or in a controlled solvent vapor atmosphere, and a DC voltage was applied. For high molecular weight polymers temperature annealing is impractical because of their high melt viscosities. Solvent vapor annealing on the other hand, very effectively increases the polymer mobility at low temperatures, significantly reducing the thermal degradation of the polymer. Similar to the well–documented results using homopolymer films, the application of an electric field across a liquefied block copolymer–air bilayer leads to an array of polymer pillars that span the two electrodes. The pillars with a characteristic center to center distance are the result of the electrostatic pressure that overcomes the surface tension of the polymer–air interface.

Figure (7.2) shows the pattern formation on the micrometer scale of PS–PMMA block copolymers with two different molecular weights. The diameter and lateral positions of the columns are replica of the design pattern of the top electrode. The two annealing protocols (heating (a) and swelling in solvent vapor (b,c)) produced comparable results.

In difference to the EHD pattern formation of homopolymer films, the micrometer–sized block copolymer pillars reveal a 10–nm sub–structure in the high–resolution SEM images in Fig. (7.3). These images are taken after degradation of the PMMA component with UV light and subsequent rinsing with acetic acid and Millipore water. They show individual high–aspect ratio sheets of lamella which are perfectly aligned parallel to the axis of the pillars, along the orthogonal field lines. The gaps in the polymer morphology arise from defects and/or mechanical instability of the remaining high aspect ratio lamellar sheets which were unable to remain perpendicular to the substrate after removal of the PMMA component. Only PS lamellae that extend down to the substrate survive the PMMA degradation and washing step. Interestingly, our finding that the standing lamellae extend down to the substrate is new, compared to the results of Xu *et al.* [128], reporting that surface induced parallel preferential orientation of some surface–near lamellae dominates over the electric field alignment.

The in–plane arrangement of lamellae is intrinsically anisotropic. The confinement into columns therefore leads to the three different in–plane assemblies schematically shown in Fig. (7.1): onion–type concentric alignment of lamellae (Fig. (7.3a), arrow), bent lamellae pointing towards the column mantle, Fig. (7.3b) and parallel sheets (book sheets), Fig. (7.3c). The in–plane orientation of the lamellae is the result of an interplay between surface interactions, electric field alignment during column formation, bending energy of the lamellae, and the energy associated with defects in the lamellar structure.

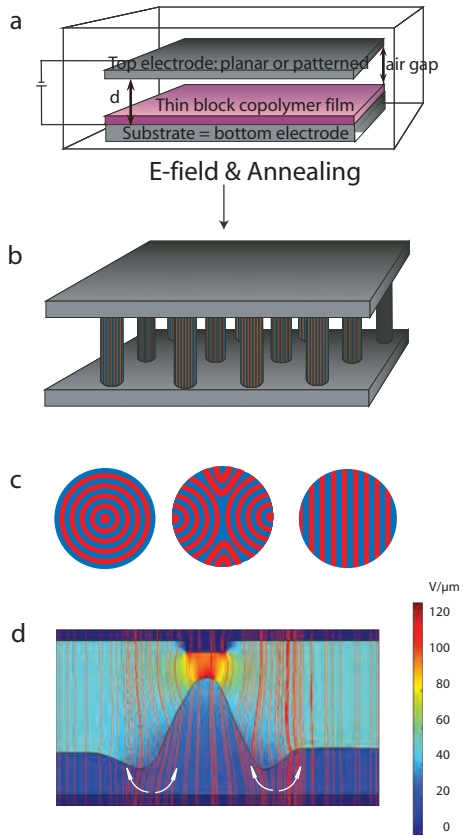

Figure 7.1: . *Schematic drawing of the experimental procedure. (a) Experimental setup of the EHD pattern formation experiments. The outer box represents the atmosphere of the experiment which is either a $T > T_g$ of the block copolymers or a controlled solvent vapor atmospheres. The sample chamber contains a block copolymer film supported by a silicon wafer and a top electrode which is placed above the polymer film leaving an air gap. A voltage is applied between the electrodes while the sample is annealed. (b) EHD pattern formation: columns span the two electrodes. The columns have an internal structure consisting of lamellar microdomains which are aligned perpendicular to the electrodes and parallel to the electric field vector. (c) Schematic cross–sections through the columns of (b) showing three possible in–plane configurations of the lamellar microdomains. (b) Simulation representing the field distribution in an intermediate stage of the EHD structure formation of a polymer film. The simulation shows an initially 700 nm thick PS layer with a dielectric constant of 3.4 in a capacitor with a plate spacing of 2 µm and an applied voltage of 80 V. The pattern is induced by a 400 nm wide, 150 high central protrusion on the 4.2 µm wide top capacitor plate. The image clearly shows the lateral component in the field lines.*

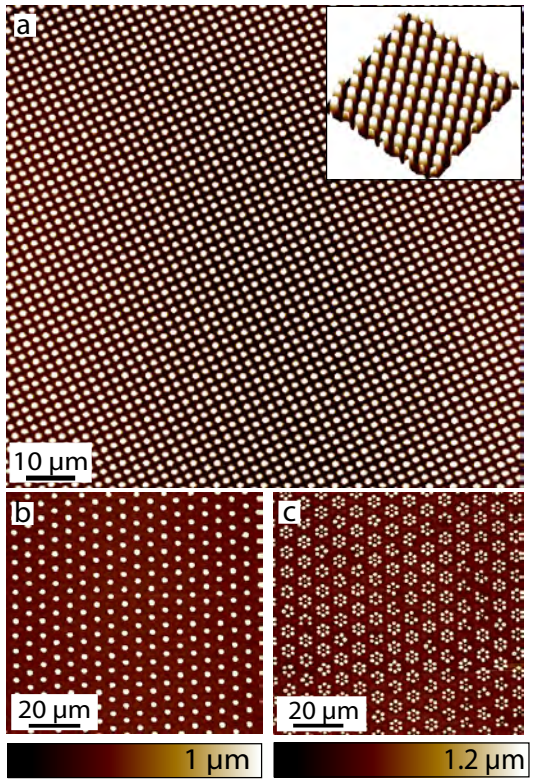

Figure 7.2: *AFM images of micrometer–sized patterns of PS–b–PMMA films made by EHD lithography. (a) P(S–d8)$_{31}$–b–PMMA$_{31}$ film with an initial film thickness of 135 nm. The block copolymer film was annealed at (170 °C under an applied electric field of 40 V/m for 19 hours. The diameter of the pillars, ≈ 1 µm in size and the inter–pillar spacing of 2 µm were controlled by a topographically structured top electrode. The height of the pillars is around 410 nm. The inset shows a three dimensional view of the pillars. (b) and (c): Micropatterns of PS$_{33}$–b–PMMA$_{32.5}$. A 94 nm thick film was swollen at* $p/p_{sat} = 0.85$ *in toluene vapor for 15 minutes, and a voltage of 80 V was applied across the electrodes for 17 hours. The patterned films were subsequently slowly dried by reducing the ratio p/psat down to 0 (pure nitrogen) in 17 steps of 30 sec each, i.e. the film was dried very slowly. The samples were additionally dried with pure nitrogen for 5 minutes before removing the electric field. (b) AFM image of 2 µm wide and 660 nm high columns. The pattern sizes match the dimensions of the structured top electrode. (c) AFM image of ≈ 1 µm high columns.*

In particular, the small difference in PS and PMMA surface energies favors the parallel alignment of the lamellae at the column mantle. This is opposed by the in–plane components of the electric field during the intermediate stages of column formation. This effect is visualized by the outward bent field lines in the simulation of Fig. (7.1d). The third free energy contribution arises from the bending of the lamellae, leading

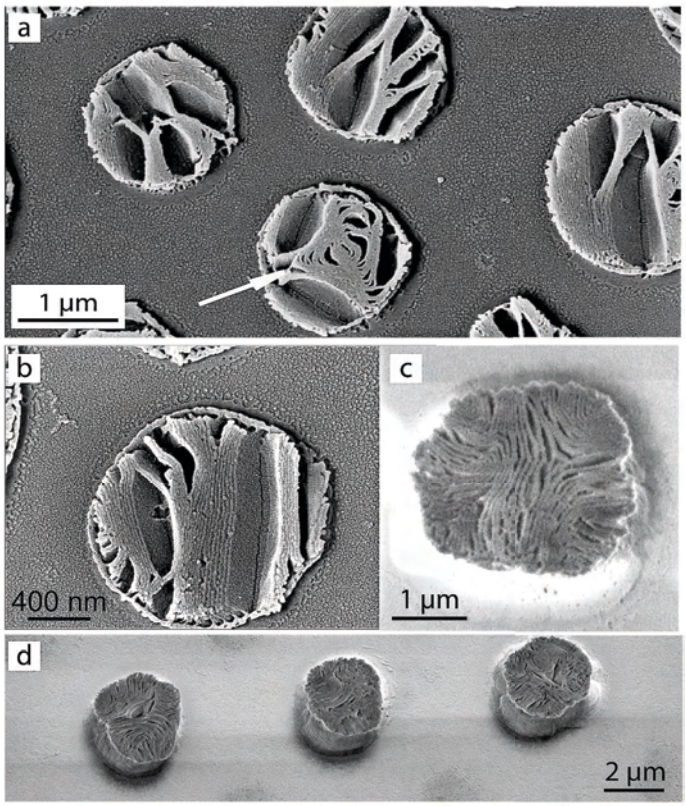

Figure 7.3: *SEM images of the microphase morphology of PS–b–PMMA columns showing complete alignment of the lamellar microdomains normal to the substrate. The pillars were exposed to UV–light and rinsed in acetic acid and water to remove the PMMA phase. Before imaging, the films were coated with a 5 nm thick layer of gold. (a) and (b) Top view of pillars of P(S–d8)$_{31}$–b–PMMA$_{31}$ formed at 170°C with an applied voltage of 40 V for 22.5 h. Before removing the electric field, the samples were cooled down to room temperature. The initial film thickness was 135 nm, the air gap was 235 nm. The height of the pillars is 370 nm as measured by AFM. (c) and (d): Top view of PS$_{89}$–b–PMMA$_{95}$ pillars. The initially 170 nm thick film was swollen for 20 minutes at* p/p_{sat} *= 0.85 in toluene vapor and a voltage of 80 V was applied across the capacitor plates for 4.5 hours. After drying the patterned films in pure nitrogen for 30 minutes, the electric field was removed. In the dry state, the columns are 2.5 µm high.*

to a frustration of the polymer conformations, which also penalizes the formation of defects in the lamellar morphology.

The relative importance of these three free energies gives rise to the different in-plane morphologies in Fig. (7.1c). The onion morphology is favored by a lowering of the surface energy, overcoming the lateral component in the electric field. The opposite case, that is, the dominance of the lateral field components over the reduction of

surface free energy leads to the conformation of outward pointing lamellae (Fig. (7.1c, middle). Both conformations cause, however, the bending of lamella in the interior of the column and, because of polymer frustration, result in the formation of defects in the lamellar structure. The minimization of lamellar bending is the dominant effect for the book–sheet morphology, which has a non–homogeneous mantle boundary.

Interestingly, all three possible configurations are found, often on the same sample, irrespective of the type of annealing protocol and polymer molecular weight. While it is possible that the in–plane microphase morphology is not fully equilibrated, this is unlikely, given the fact that the lamellae are fully aligned along the column axis and the qualitatively similar results for both polymer molecular weights and annealing methods. This indicates that none of the free energies responsible for the three in–plane alignment described above is dominant, leading to strong fluctuations between them.

Careful examination of the SEM images in Fig. (7.3) reveals the interplay of opposing free–energy contributions in close vicinity of the mantle. Most columns are surrounded by a single PS lamella, with the further inward lamellae pointing perpendicular to the mantle. This indicates that surface tension dominates the short–range morphology, while the longer ranged electrostatic forces dominate the lamellar arrangement in the near–mantle region further inside the column. The free energy associated with the bending of the lamellae and the creation of grain boundaries seems to be small in comparison, since all columns exhibit (sometimes elaborate) defect structures.

7.3.2 Block copolymer EHD alignment in columnar structures

Periodic columns made of polystyrene–block–polymethylmethacrylate (P(S–d8)$_{31}$–*b*–PMMA$_{31}$) spanning the distance between the two electrodes were spontaneously - formed by temperature annealing the sandwich above the glass transition temperature of the constituent copolymer blocks and applying an external electric field. The electrostatic pressure exceeds the capillary pressure induced by the curvature of the liquid film. As a consequence, the block copolymer flows primarily in lateral direction, parallel with the substrate, amplifying the existent capillary waves with a characteristic lateral wavelength on micrometer scale. An overview of a small area covered with amplified capillary waves, in their early stages is given in Fig. (7.4a). The SEM images from Fig. (7.4) were taken after degrading the PMMA component, revealing only the PS component. On the macroscopic scale, the electrohydrodynamic field destabilizes the block copolymer–air interface, while on microscopic scale, structure formation is determined by a competition between microphase separation (in the strong segregation limit), substrate induced alignment, alignment along the electric field lines (orthogonal to the substrate), and orientation process induced by the flow of the material into the columns (in–plane flow). While it is theoretically hard to predict which of the four mechanisms is predominant during the early stages of film destabilization, the SEM images indicate that the block copolymer adopts a "worm—like" PS morphology as a compromise between all the competing factors. This morphology is possible a kinetic intermediate stage rather than an equilibrium phase for temperatures below

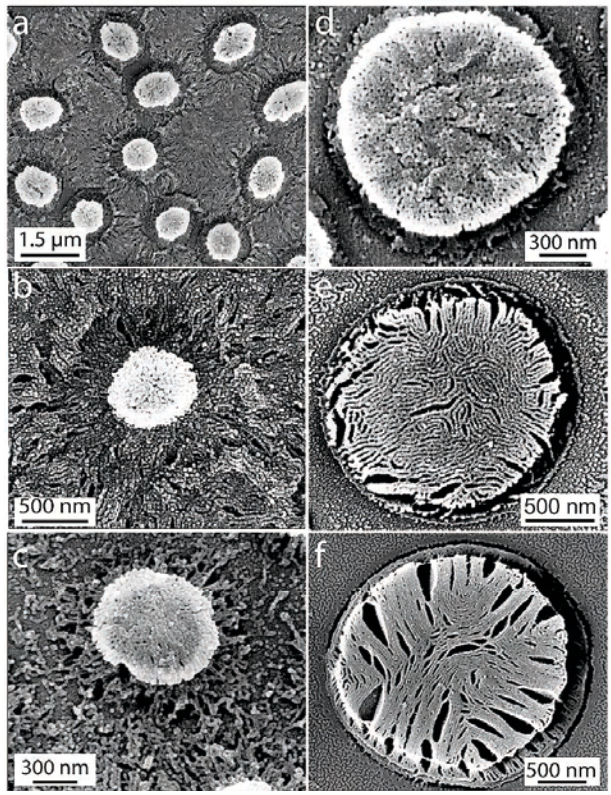

Figure 7.4: *SEM images showing the evolution of the column growth with time. On macroscopic scale, (a)–(f) images show the electrohydrodynamic column formation. On microscopic scale, the block copolymer molecules simultaneously and continuously align from a poorly ordered state towards the formation of completely phase separated lamellae sheets.*

the order–disorder transition. These structures are connected to the substrate and no evidence for layering parallel to the substrate is found. The high–magnification images in Fig. (7.4) reveal that the electrohydrodynamic process triggers not only the formation of micrometer sized pillar like structures, but also initiates the formation of the equilibrium lamellar microphase morphology from the initially poorly ordered state. Figure 7.4 shows the progress of the micrometer pillar formation and the simultaneous alignment of the copolymer blocks. The images in Fig. (7.4a–c) show the formation of a cylinder from the initially flat film ($h \approx 140$ nm) after annealing for 20 minutes at 170 °C with an applied voltage of $U = 40$ V at different locations on the sample. To follow the mechanism of the block copolymer alignment within the column, it is interesting to focus our attention first on a single column and its surroundings. Figure (7.4b) shows the image of a pillar that did not span the two electrodes as indicated by its rounded shape and the material at the film adjacent to the pillar. In the

process of the pillar growth, the material is drawn upwards and the area surrounding the structure is depleted. While in Fig. (7.4b) the surrounding area is almost completely covered with a worm-like morphology showing a high degree of alignment in the direction of the flow towards the pillar. A larger depleted area and therefore a bigger pillar is shown in Fig. (7.4c), while Fig. (7.4d) shows a complete pillar identified by shape (well defined core and flat top) fully spanning the two electrodes. At this stage a top view does not reveal any information regarding the formation of lamellar sheets within the pillar,but the flow of material into the column seems to have induced a vertical alignment of the worm-like morphology. At this stage, the flow of material is complete and further alignment of the copolymer morphology can only occur by the orientation of the blocks under the influence of the electric field. Due to the dielectric contrast between the blocks, the microdomains tend to orient parallel to the electric field vector, thereby lowering the energy of the system. In Fig. (7.4e) the presence of the lamellar morphology can already be identified and several in–plane defects are visible. Figure (7.4f)shows the fully formed lamellar sheets penetrating down to the substrate, exhibiting a reduced number of in–plane defects.

7.3.3 Block copolymer EHD alignment in arrays of lines

Here, we concentrate on the electrohydrodynamic alignment of symmetric block copolymers. The overall process of block copolymer pattern formation and alignment is guided by pre–patterned doped silicon electrodes consisting of an array of lines. The pre–patterned lithographic features possibly provide a means for the local registration of the self assembled block copolymer morphology in micrometer-sized structures. By using block copolymer materials, the large features are sub–divided into sublithographic units on the nanometer scale. Fig. (7.5a) shows an SEM image of early stage block copolymer pattern formation. The liquid block copolymer film ($h \approx 140$ nm) was exposed for 15 minutes to a potential difference between the pre–patterned electrode and the substrate of 60 V. During the temperature annealing process (170 °C) in the presence of the externally applied electric field, columns appeared under the downward protruding lines. The SEM image reveals the direction of polymer flow. The high resolution image indicates that the block copolymer molecules form a worm-like morphology , which aligns in in the flow direction that gives rise to the emerging EHD structure. More detailed indications of the flow induced alignment can be visualized in a later stage of the pattern formation, when the columns grow and start to coalesce, Fig. (7.5b). As the columns grow they draw in more and more material from the surrounding film, touch the top electrode, coalesce laterally, and form a positive replica of the pre–patterned electrode. During this process, the block copolymers align both in the direction of the flow and in the electric field. In Fig. (7.5c) the block copolymers are vertically pre–aligned within the line microstructures, showing an intermediate stage of the process. A complete alignment of the blocks takes place when the mesoscopic replication of the lines is complete and all the material from the surrounding film is depleted, Fig. (7.5d). The image reveals lamellar sheets within the micro–lines that run from top to bottom of the lines, perpendicular to the substrate, through the

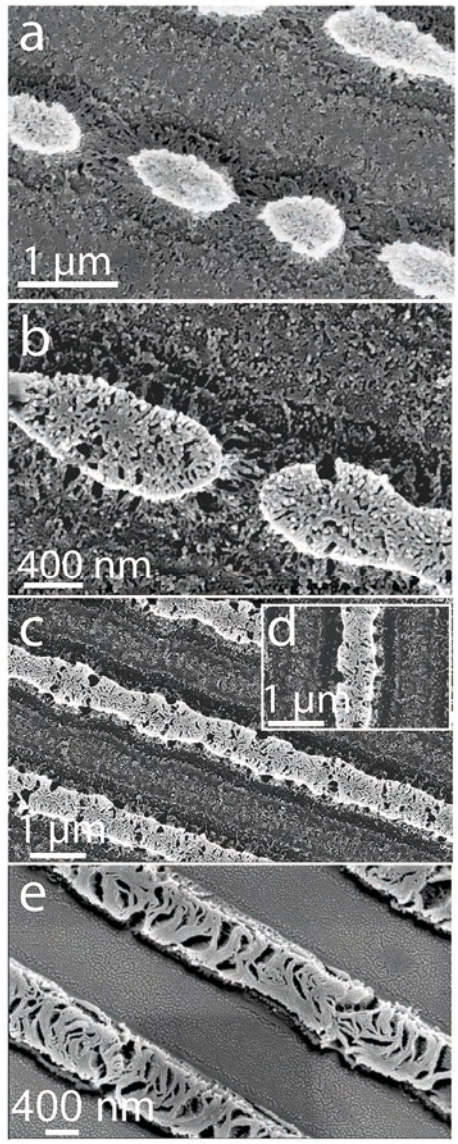

Figure 7.5: *Block copolymer EHD alignment in arrays of lines. The SEM images from (a)–(e)show the evolution of line patterns replicated by the electrohydrodynamic instability with time. On microscopic level, the block copolymer molecules continuously align from a poor ordered state towards a completely phase separated state in which they form lamellar sheets pointing towards the side walls of the lines.*

entire micrometer sized line. These self assembled lamellar sheets tend to point towards the side walls and not lie along the axis of the lines. The in–plane orientation of the lamellar domains is therefore guided mainly by the lateral components of the electric field which is introduced by the presence of the pre–patterned silicon electrodes used in this study. The highest electric field is concentrated in the gap between the protruding silicon lines and the polymer surface, Fig. (7.1d). Once the polymer lines have fully formed, the highest field gradients are at the side walls of the block copolymer lines. Here, the strength of the in–plane and orthogonal component of the electric field are comparable. However, the in–plane electric field in the line decreases towards the center of the line. We therefore believe that the in–plane alignment of the lamella starts at the side walls and propagates towards the center of the line, giving rise to a new mechanism of block copolymer alignment.

7.3.4 Other topological transitions: coalescence of columns during EHD pattern formation

Figure (7.6) shows the coalescences of some columns during EHD pattern formation. The coalescence corresponds to a late stage of the EHD pattern formation. In Fig. (7.6a), the block copolymer columnar structures made contact with the upper electrode, grew in diameter and merged together with one or more neighboring columns. A more detailed explanation of the coalescence process is given in Chapter 4.

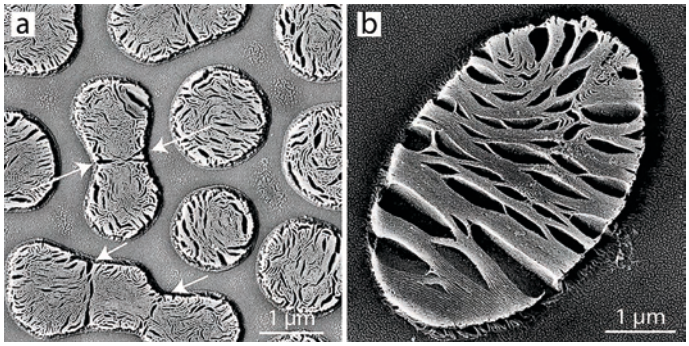

Figure 7.6: *Electrohydrodynamic pattern formation in symmetric block copolymers. The SEM images reveal the coalescence of columns (a) The arrow indicate the position at which the coalescence occurs. The alignment of the block copolymers within the coalesced structures is not much disturbed (b) In later stages of the coalescence, the in-plane alignment of the block copolymer components is strongly influenced by the shape of the structure. In the middle of the elongated structure, where the curvature of the core is minimal, the block copolymers form almost perfect parallel, book–like sheets.*

7.4 Conclusions

In summary, we demonstrate a combined bottom–up and top–down approach based on electrohydrodynamic formation of surface patterns in thin films and the self–assembly of symmetric block copolymers within these patterns. Upon temperature or solvent–vapor annealing, initially flat lamellar block copolymer films are destabilized by electric fields leading to the formation of micrometer–sized pillars perpendicular to the substrate. Within each pillar the lamellar block copolymer domains are aligned parallel with respect to the pillar axis. The formation of the patterns on the two different length scales is explained in terms of the interplay of molecular self-assembly and the structural control exerted by electrostatic forces. The structures formed on the micrometer length scale by the electrohydrodynamic instability compartmentalize the block copolymer microphase morphology. Three different in–plane morphology alignments are observed which result from a complex interplay between the electrohydrodynamic forces, confinement and curvature of the pillars. The in-plane morphology is a result from an interplay between the surface tension of the constituent blocks, electrostatic force and the frustration of polymer conformation caused by lamellar bending. By choosing ridges and pillars on a patterned mask, we have guided the development of micrometer structures along a design pattern. Within linear ridges and pillars, the microphase-separated domains have shown interesting in–plane orientations, which are be dependent on the shape of the geometrical confinement. By enabling the pattering of block copolymer films on two different scales simultaneously may open a path towards fabrication of functionalized devices for electronic, chemical and biological applications. Further study, both theoretical and experimental will be necessary to understand fully the influence of the various geometric confinement in guiding these structures.